Discrete Events of Ionosomes at the Water/Toluene Micro-Interface

Jingyan Zhang,[a] Linhan Huang,[a] Taoxiong Fang,[a] Feng Du,[a] Zhipeng Xiang,[b] Jingcheng Zhang,[a] Ran Chen,[c] Pekka Peljo,[d] Gangfeng Ouyang,[a] and Haiqiang Deng*[a]

Dedicated to Professor Hubert H. Girault on the occasion of his 65th birthday.

[a] J. Zhang, L. Huang, T. Fang, F. Du, J. Zhang, Prof. Dr. G. Ouyang, Prof. Dr. H. Deng
School of Chemical Engineering and Technology
Sun Yat-sen University
Zhuhai 519082, China
E-mail: denghq9@mail.sysu.edu.cn

[b] Dr. Z. Xiang
Guangdong Provincial Key Laboratory of Fuel Cell Technology, School of Chemistry and Chemical Engineering
South China University of Technology
Guangzhou 510641, China

[c] Prof. Dr. R. Chen
School of Chemistry and Chemical Engineering
Southeast University
Nanjing 211189, China

[d] Prof. Dr. P. Peljo
Research Group of Battery Materials and Technologies, Department of Mechanical and Materials Engineering, Faculty of Technology
University of Turku
20014 Turun Yliopisto, Finland

Supporting information for this article is given via a link at the end of the document.

Abstract: Emulsification is a powerful technique for dispersing one fluid (water or oil) in the form of tiny droplets within an immiscible continuous fluid (oil or water). Hence, emulsion is an essential component of medicine, food, and shampoo, to name a few. An emulsifier, e.g., a surfactant, is normally added inside emulsions to stabilize the water/oil interfaces. Ionosomes, nanoscopic water droplets enclosed solely by an ionic bilayer, in which one layer formed from small and more mobile hydrated ions residing in the inner aqueous side and another layer formed from lipophilic bulky counter-ions riveted tightly in the adjacent outer oil side, were generated and in-situ counted "one at a time" at a polarized water/toluene micro-interface. Chemical polarization via the biphasic distribution of an antagonistic salt proved the proposed ionic bilayer structure of ionosomes. Promotion effect on Li^+–ionosomes revealed by single-entity electrochemistry for quaternary ammonium cations with different alkyl chain length and with different concentration sheds new light on the mechanism of ionosomes. Fusion of a Li^+–ionosome with the polarized soft micro-interface follows the bulk electrolysis model.

Introduction

Water-in-oil (w/o) emulsions are composed of tiny water droplets that are dispersed homogeneously into a continuous oil phase (functioning as the main fluid, by volume ratio). This structure is used for the delivery of hydrophilic compounds, which has found numerous applications in pharmaceutical, agricultural, cosmetic, and

food industries.[1] However, a surfactant, an amphiphilic molecule containing both a hydrophilic group (i.e., its polar head) and a hydrophobic group (i.e., its nonpolar tail), is added to form a physical barrier that prevents the suspended droplets from coalescing and breaking the emulsion. According to the composition of its head part, surfactants are classified into three categories: non-ionic, ionic, and amphoteric. An ionic surfactant dissociates into an amphiphilic ion and a small inorganic counterion. For a w/o emulsion, this amphiphilic ion adsorbs at the water/oil interface with its polar head group facing the water and its nonpolar tail extending outward into the oil. Accordingly, the interfacial tension is lowered, stabilizing the droplets, besides the electrostatic repulsion mechanism due to the net charge carried on its polar head.

Similarly, the antagonistic or polar salts, typically composed of small inorganic cations/anions and bulky organic counter-anions/cations, display surfactant properties at a water/oil interface.[2] Classical examples of antagonistic salts include sodium tetraphenylborate and lithium tetrakis(pentafluorophenyl)borate (LiTB, Scheme 1).

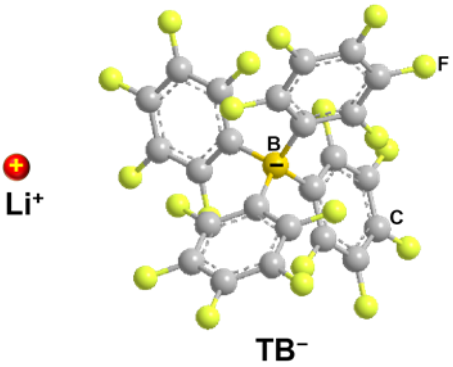

Scheme 1. The molecular structure of the antagonistic salt, Li^+ (left) and TB^- (right).

Clustering of water molecules in hydrophobic organic solvents can be stabilized by an ionic bilayer, i.e., one hydrophilic ionic layer at the aqueous side and one organic layer of bulky counter-ions at the oil side, which are formed by electrostatic attraction between one another (see Scheme 2). These nanoscopic ionic-bilayer enclosed water clusters/droplets were very recently discovered and termed ionosomes, by us.[3] Ionosomes can be easily described by the (discrete) Helmholtz electrical double layer (EDL) model for the polarizable interface between two immiscible electrolyte solutions (ITIES), as proposed by Girault and co-workers in 2020.[4] The large organic ions act as immobile anchoring points generating micropotentials with the electric field lines radiating out spherically; this inhomogeneous potential can be directly compensated by the smaller, more mobile aqueous counter-ions in a one-to-one manner. This model rationalizes ionosomes as spherical ionic capacitors (formed by two concentric spheres carrying equal and opposite discrete charges) which feature a total potential drop only through the correlated ionic bilayers. In essence, each ionosome is a nanoscopic spherical polarized ITIES. Our prior single-entity electrochemistry (SEE) of ionosomes indicated that the ionosomes migrated in the electrical field. This argument was supported by the fact that ionosomes could only be detected at the potentials far negative/positive from the potential of zero charge (PZC).[3] In short, an ionosome bears a net charge: bulky organic ions cannot compensate completely the spherical electric field generated by its hydrophilic counter-ions, due to the steric limitation. Considering the high spontaneity of assembling ionosomes via either electrochemical or chemical polarization,[3] we can conclude that the potential (generated from the ionic bilayer) drops mainly through the ITIES, but with a minor component beyond the interface that is responsible for the diffuse layer. Therefore, it seems that the Gouy-Chapman EDL model is

more applicable for the ITIES polarized by ions. Certainly, clarification of this pivotal issue regarding the EDL structure of the polarized ITIES requires further theoretical and experimental investigations.

In our prior work, with SEE, we only observed the discrete collision/fusion events of single ionosomes at both the water/α,α,α-trifluorotoluene (TFT) and the water/1,2-dichlorobenzene (DCB) interfaces, rather than at the water/1,2-dichloroethane (DCE) and the water/5-nonanone interfaces.[3] The dielectric constants (at 20 °C) of the aforementioned four organic solvents are 9.18, 9.93, 10.36, and 10.60, respectively, indicating a slightly lower energetic penalty for charge separation/dissociation in the latter two media. Hence, it is slightly more difficult to wrap/stabilize an ionosome with an ionic bilayer from an antagonistic salt in either DCE or 5-nonanone. Note that the widths of the polarizable potential window (PPW) obtained at both the water(LiCl)/TFT(BATB) and the water(LiCl)/DCB(BATB) interfaces, are similar, being 1.1 V; while, PPWs at the water(LiCl)/DCE(BATB) and the water(LiCl)/5-nonanone(BATB) interfaces, are 0.8 and 0.45 V wide, respectively.[3] BATB abbreviates for bis(triphenylphosphoranylidene)ammonium tetrakis(pentafluorophenyl)borate, and is used as a lipophilic supporting electrolyte. This implies that the Gibbs energy of transferring hydrated ions into an immiscible organic medium plays a pivotal role in driving the self-assembling of ionosomes. The PPW width reflects the solubility of water in these organic solvents: Water is insoluble in both TFT and DCB, but is quite soluble in both DCE[5] and 5-nonanone (see Justification, on page S2, in the Supporting Information (SI), where the solubility of water in toluene is also discussed). Because in an electrical field, small hydrated ions transfer into an immiscible organic medium by a dynamic formation/break of a water chain/finger mechanism.[6] The higher water content in an organic medium favors interactions of electrostatics and/or hydrogen bonding between water clusters located at the oil side of the ITIES and water fingers formed during a highly hydrophilic ion transfer (IT),[7] thus lowering the energy barrier for IT. Intuitively, it is easier to reach supersaturation of water in both TFT and DCB, which is beneficial for formation of ionosomes. In this sense, we expect that self-assembly of ionosomes requires organic media with (1) lower dielectric constant, and (2) lower solubility of water.

Compared to the four organic solvents aforementioned, toluene is frequently used for preparation of oil-in-water (o/w)[8] or w/o[9] emulsions and also in the Brust-Schiffrin biphasic synthesis of thermally and air-stable monodisperse gold nanoparticles with controlled size.[10] It is known that toluene is an apolar organic solvent with a low dielectric constant of 2.38 and features with a solubility of water in itself of 0.033% (mass percentage) at 25°C. The high resistance of low dielectric-constant media like toluene has greatly restricted electrochemical studies of various ionic analytes of interest at the ITIES between water and toluene. This fact results in a very small amount of literature that is available for the ITIES electrochemistry at water/toluene interface.[11] In the present work, we have extended the scope of SEE of ionosomes formed and detected to a micro-ITIES between water and toluene, proving the universality of ionosomes, viz., nanosized water droplets enclosed solely by ions. This work expands the range of organic solvents that can be used and provides new physical insights into the assembling mechanism of ionosomes.

Results and Discussion

The electrochemical generation and detection of Li^+–ionosomes are illustrated in Scheme 2 and explained in its caption. Briefly, a positive bias (vector E in black) applied at a water/toluene micro-ITIES drives hydrated Li^+ transfer from water into toluene for assembling Li^+–ionosomes via the Coulombic attraction between Li^+ and

lipophilic counter-ion TB^-. Water molecules either dragged by Li^+ or dissolved inside toluene participate in the assembly of Li^+–ionosomes. The relative length of an arrow between a Li^+–ionosome and its component indicates the favorable propensity towards assembly of water clusters. In essence, it is the electrochemical way of preparing an antagonistic salt in organic medium, followed by its self-assembly into an ionosome. Under a reversed electric field (vector E in orange), a single Li^+–ionosome collides and fuses with the interface, resulting in a discrete and downward Li^+ ion transfer spike.

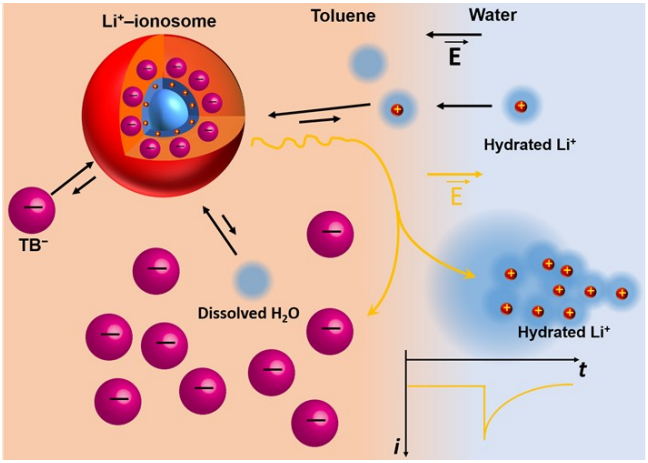

Scheme 2. Schematic diagram of the Li^+–ionosome (not to scale) formed by electrochemical polarization and its ensuing fusion with the toluene/water micro-ITIES, leading to release of the hydrated Li^+ cations into the water phase. The *i*–*t* trace records a downward spike for this event. The molecular structure of the bulky and lipophilic TB^- is detailed in Scheme 1. Note that the electric field direction for formation (vector E in black) and detection (vector E in orange) of the Li^+–ionosome is exactly opposite.

The next step is to prove the concept experimentally. A hydrophilic salt like LiCl and a hydrophobic salt like tetradodecylammonium tetrakis(pentafluorophenyl)borate (TDDATB), distributed in aqueous and another immiscible organic phases, respectively, render the ITIES polarizable. Specifically, a background cyclic voltammogram (CV) with a PPW of ~0.9 V (from –0.05 to +0.85 V) is obtained and shown in Figure 1, using the electrochemical cell 1 (*X* = Li) detailed in Scheme 3. A micropipette with a typical inner diameter (i.d.) of ca. 2 µm (e.g., 2.1 µm, see Figure S1, SI) was used throughout this work for SEE of ionosomes. Similarly, Figure 1 shows PPWs of ~0.85 and 0.75 V, respectively, measured for the cell 1 with aqueous electrolyte either of 10 mM NaCl or $MgCl_2$ or of 10 mM KCl or NH_4Cl (see Scheme 3). Note that K^+ transfers at a slightly more positive potential than that of NH_4^+, which aligns well with both our previous experiments conducted at the water/TFT interface[3] and the results obtained at the water/toluene interface by Kasuno et al.[11c] Note that Mg^{2+} transfers at a lower Galvani potential than that for Li^+ but at a marginally higher value than that for Na^+. This differs from observations made by Kasuno et al.,[11c] possibly due to the difference in the lipophilic supporting electrolytes employed by us and them. Ion-pairing at the toluene side of the ITIES is more pronounced for Mg^{2+} transfer, which is evidenced by a strong negative peak current during the reverse scan. This negative peak current could be caused by dissociation and/or desorption of ion-pair, namely Mg^{2+}–$(TB^-)_2$, from the toluene side of the ITIES, followed by ensuing Mg^{2+} transfer back into water. Ion-pairing facilitated Mg^{2+} transfer supports the shuttling mechanism of hydrophilic IT proposed by Mirkin and co-workers.[12] This explains the anomalous thermodynamics behavior of Mg^{2+} with respect to Li^+ during their transfers. The fact that a shift at the positive limit/end of PPW with variation of aqueous cations and the independence of the negative limit of PPW on Cl^- imply that the PPW is controlled mainly by the transfer of Cl^- and hydrated cations like Li^+ from water to toluene at negative and positive potentials (i.e., water vs. toluene), respectively. Negative limit of the PPW by Cl^- is

further supported by the potential shift on aqueous LiCl concentration (Figure S2, SI), in which the onset potential for Cl^- transfer shifts positively with the increasing aqueous LiCl concentration. As expected, the onset potential for Li^+ transfer shifts negatively with the increase in LiCl concentration. Specifically, when LiCl increases in concentration from 10 to 100 mM, the positive end of the PPW moves to the left by ~70 mV, and the negative end of the PPW moves to the right by ~49 mV, which is basically in line with the theoretical value (approximately ± 59 mV/10-fold concentration), according to the Nernst equation (Eq. 1):

$$\Delta_{\mathrm{o}}^{\mathrm{w}}\phi = \Delta_{\mathrm{o}}^{\mathrm{w}}\phi_i^{\circ} + \frac{RT}{z_i F}\ln\left(\frac{a_i^{\mathrm{o}}}{a_i^{\mathrm{w}}}\right) \qquad (1)$$

where $\Delta_{\mathrm{o}}^{\mathrm{w}}\phi$ is the Galvani potential difference, $\Delta_{\mathrm{o}}^{\mathrm{w}}\phi_i^{\circ}$ is the standard transfer potentials of *i* (*i* represents ion), *R*, *T*, *z*, *F*, and *a* are the gas constant, thermodynamic temperature, charge number of *i* including the sign, Faraday constant, and activity of *i* in phase o (i.e., toluene) or w (i.e., aqueous), respectively. To simplify the complexity, we used concentration *c*, instead of *a*, for a first approximation. Note that when LiCl concentration is increased from 100 to 1000 mM, the positive end of the PPW moves to the left by ~90 mV, and the negative end of the PPW moves to the right by ~78 mV, which is somewhat larger than the theoretical value. This slight discrepancy might stem from both the non-negligible uncompensated *iR* drop in toluene as the ionic current increases and the use of concentration instead of activity especially at high concentrations. In brief, evolution of the limits of the PPW as a function of the aqueous electrolyte concentration conveniently helps us to determine which ionic species limit each edge of the PPW. Nevertheless, the potential shift effect discussed above is only apparent and in essence, only the foot of the wave is recorded and the apparent shift is an increase of the current due to the increase of the aqueous ion concentration. Besides, when Li_2SO_4 is used instead of LiCl as the aqueous electrolyte, SO_4^{2-} transfers at more negative potential than that of Cl^-, leading to a wider PPW (green trace, Figure S2, SI).

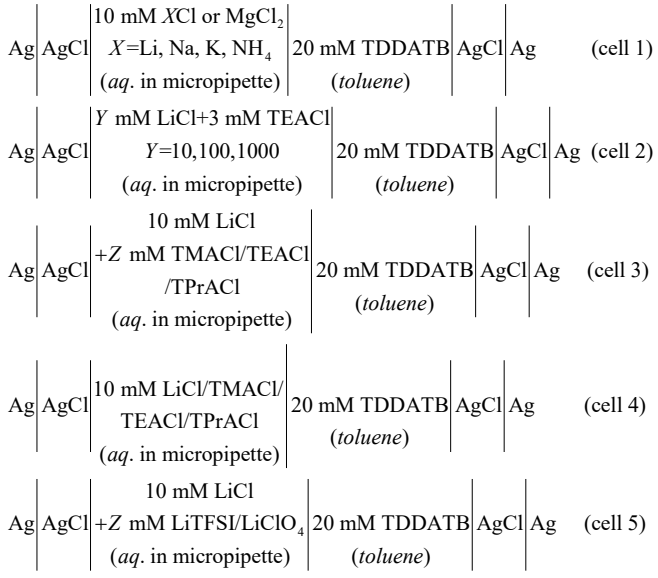

Scheme 3. The electrochemical cell composition.

Based on the above results, 10 mM LiCl and 20 mM TDDATB were used as the supporting electrolytes for aqueous and toluene phases throughout the subsequent experiments.

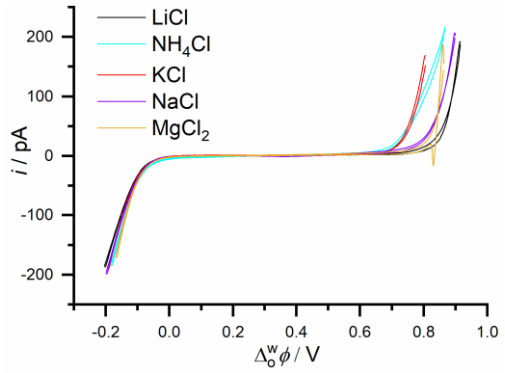

Figure 1. CVs measured at a micropipette (inner diameter: 2.0, 2.1, 2.0, 1.9, and 2.1 µm, respectively) supported ITIES between water of either 10 mM LiCl (black trace), or $MgCl_2$ (yellow trace), or NaCl (violet trace), or KCl (red trace), or NH_4Cl (cyan trace) and toluene of 20 mM TDDATB, using the electrochemical cell 1 (Scheme 3). Scan rate of CV: 20 mV s^{-1}.

Figure 2 shows steady-state CVs of simple IT of different quaternary ammonium cations at varied concentrations. The diffusion-limited steady-state plateau current (i_{ss}) in the CVs for transfer of either tetramethylammonium (TMA^+), or tetraethylammonium (TEA^+), or tetrapropylammonium ($TPrA^+$) is proportional to the concentration of each ion in the range of 1–5 mM (Figure 2, panels B, D, F). This linear relation obeys the following equation (Eq. 2) for ion egress from the micropipette under steady-state control.[13]

$$i_{ss} = 4f(\theta)z_i F D_w c_w r \qquad (2)$$

In Eq. 2, $f(\vartheta)$ is a function of the tip taper angle, ϑ,[14] r is the inner radius of a micropipette tip assuming an inlaid disk geometry, D_w and c_w are diffusion coefficient and concentration of ions in the bulk aqueous solution, and z and F have been defined before. The ϑ is the angle between pipette inner wall and central axis, varying from 0 to $\pi/2$. Accordingly, $f(\vartheta)$ is essentially a normalized steady-state current, which increases from 0 to 1 as ϑ scans from 0 to $\pi/2$.[14] In our case, $f(\vartheta)$ is ≤ 0.1, considering the small taper angle of our pulled typical micropipettes, which are shown in Figure S1, in SI. Interestingly, almost retraced steady-state current behaviors for both forward and backward branches in CVs were observed (Figure 2, A, C, E). The CVs record transfer of ions that are initially located inside the micropipette that features with a small tip taper angle. Steady-state CVs of simple IT crossing the ITIES were also observed at both nanopipettes[15] and micropipettes[3, 16] by Shao and co-workers and also by us. The slope shown in the legend of Figure 2, B, D, F implies the relative magnitude of D_w of these three quaternary ammonium cations, following the sequence $TMA^+/TEA^+ > TPrA^+$. Wandlowski et al. reported a slightly smaller D_w of TEA^+ (9.3×10^{-10} m^2 s^{-1}), compared with that for TMA^+ (9.5×10^{-10} m^2 s^{-1}).[17] The anomaly of D_w between TMA^+ and TEA^+ might be understood by the fact that TMA^+ drags along more water molecules than that by TEA^+ into toluene. This is in accord with the fact that TMA^+ (radius of 283 pm) is smaller than TEA^+ (radius of 343 pm),[18] rendering the former one more hydrated. Transfer of relatively bulky ions from the confined space into the outer free space might also result in this discrepancy between us and Wandlowski et al. Nevertheless, this issue will not impact on our key findings discussed vide infra. Note that $TPrA^+$ is the largest among the three ions, with the radius of 381 pm.[18] The downward ionic spikes occurred at Galvani potentials (≤ 0.1 V for Figure 2A; ≤ 0.15 V for Figure 2C) that are more negative than PZC in the presence of either TMA^+ or TEA^+ is a collateral evidence to support the "nucleation promoter" mechanism proposed in our prior work.[3] Briefly, during the potential scan in recording a CV, TMA^+ or TEA^+ transfers across the water/toluene interface prior to Li^+, following the electric field. Water molecules dragged by either of the two (i.e., TMA^+ or TEA^+) will accumulate at the toluene side of the ITIES and finally make water supersaturated in toluene. This will promote

the nucleation and the ensuing growth of Li^+–ionosomes which are assembled via electrostatic attraction straddling the interface between hydrophilic Li^+ and lipophilic TB^-. It is the collisions and fusions of individual Li^+–ionosomes with a negatively polarized micro-ITIES (water vs. toluene) accompanying release of the hydrated Li^+ into the water phase that result in the quantized negative ionic spikes. We note that Kasuno et al. observed a similar effect of TEA^+ at the negative potential range of the PPW for the water(10 mM NaCl)/toluene(10 mM BA^+ tetrakis[3,5-bis(trifluoromethyl)phenyl]borate) micro-ITIES.[11c] However, $TPrA^+$ shows a negligible positive effect on Li^+–ionosomes generation, as evidenced by the absence of negative ionic spikes at potentials more negative than PZC on CVs (Figure 2E). A hydrophobic ion like $TPrA^+$ might cross the water/toluene interface as a bare ion, as proposed by Osakai et al.[19] The CVs without LiCl but only with a tetraalkylammonium salt are shown in Figure S3 in the SI. Clearly, no spikes are observable over the entire potential range in the absence of Li^+. It implies that hydrated Li^+ is essential for the nucleation and growth of the Li^+–ionosomes. While, the shorter-chain tetraalkylammonium cation is only a promoter.

Transfer of two anions, $TFSI^-$ and ClO_4^-, which are initially present in aqueous inside the micropipette, across the water/toluene micro-ITIES shows a similar steady-state CVs (Figure S4 in the SI). Besides, the linear relation between i_{ss} and concentration of each ion in the range of 1–5 mM is clearly seen (Figure S4, B, D, SI), although $TFSI^-$ shows a compromised correlation coefficient ($R^2 = 0.9708$) for the linear regression equation. Contrarily, all other four ions feature with a higher correlation coefficient of $R^2 > 0.99$ (refer to Figure 2 and Figure S4 in the SI). Bigger error in R^2 for $TFSI^-$ might be ascribed to the unique physicochemical properties of the LiTFSI electrolyte solutions.[20] Unlike the semi-hydrophilic cation case, $TFSI^-$ and ClO_4^- do not show any noticeable promoting effect on the generation of Cl^-–ionosomes, seen from CVs in Figure S4, A, C, in the SI. $TFSI^-$ and ClO_4^- have the ionic radii of 325 pm and 237 pm,[18] respectively. Both anions have smaller size compared to that of TEA^+, implying a higher hydration energies for the former ones.[21] It means either $TFSI^-$ or ClO_4^- can drag an equal or greater number of water molecules (with respect to TEA^+) into toluene ahead of Cl^- entry, following the electric field. Hence, we speculate that the very bulky ionic radius of $TDDA^+$ results in a significant electrostatic shielding effect of long-chain alkyl groups on the central nitrogen[22] and an inefficient correlation with the small hydrated Cl^- at the inner spherical surface of an ionosome. We have noted that the ionic radius of $TDDA^+$ is unavailable from the literature. Nevertheless, one can imagine how bulky it is, considering a radius of 415 pm for the tetrabutylammonium cation.[18] We observed a successful correlation between lipophilic BA^+ and hydrated Cl^- at the water/TFT nano-spherical interface that leads to assembling the Cl^-–ionosomes.[3] BA^+ has a radius of 650 pm;[3] therefore, $TDDA^+$ is at least bigger than 650 pm in radius. In brief, distance between lipophilic ions and their hydrated counterions locating at either side of the ITIES plays a pivotal role in assembling the ionosomes. Essentially, Coulomb's law in electrostatics, an inverse-square law, seems to govern this process. Anyway, Cl^-–ionosomes cannot be experimentally observed at the water/toluene micro-ITIES by SEE. Thus, we will focus on Li^+–ionosomes in the following investigations.

Based on the “TATB” assumption,[11c] formal ion transfer potentials in the Galvani scale for the five ions at the water/toluene interface are obtained: 0.35, 0.20, 0.05, 0.45, and 0.18 V for TMA^+, TEA^+, $TPrA^+$, $TFSI^-$, and ClO_4^-, respectively. To the best of our knowledge, it is the first reported formal Galvani transfer potential value for $TFSI^-$ at water/toluene interface. Notably, $TFSI^-$ has been extensively used as the anion in aqueous Li-ion batteries.[20a]

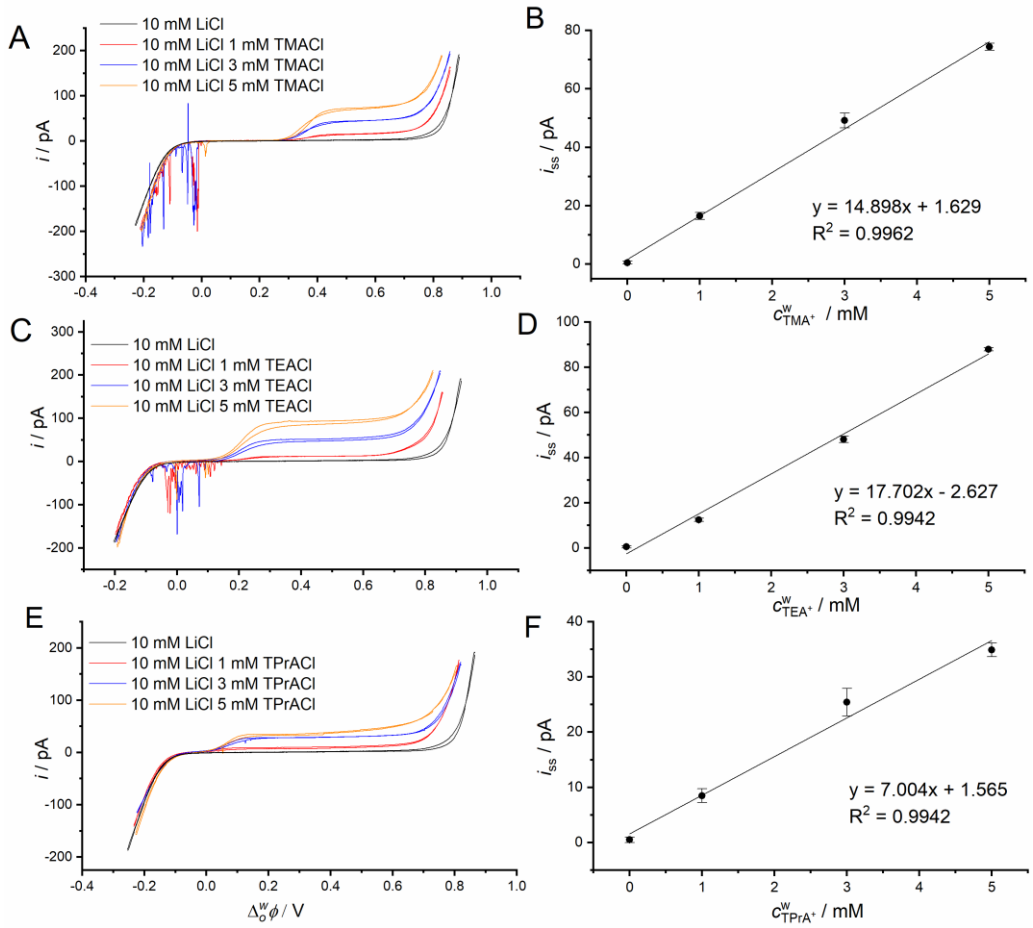

Figure 2. CVs measured at a micropipette supported ITIES between water of either (A) 10 mM LiCl + *Z* mM TMACl (*Z* = 1, 3, and 5; inner diameter: 1.8, 2.3, and 2.5 µm, for red, blue, and yellow traces), or (C) 10 mM LiCl + *Z* mM TEACl (*Z* = 1, 3, and 5; inner diameter: 2.1, 2.4, and 2.0 µm, for red, blue, and yellow traces), or (E) 10 mM LiCl + *Z* mM TPrACl (*Z* = 1, 3, and 5; inner diameter: 2.5, 1.9, and 2.2 µm, for red, blue, and yellow traces) and toluene of 20 mM TDDATB, using the electrochemical cell 3 (Scheme 3). Scan rate of CV: 20 mV s^{-1}. Note that the background CV obtained with only 10 mM LiCl in water is added in each panel for comparison, all other conditions are same as those defined in cell 1 in Scheme 3. (B, D, F) The corresponding relation between steady-state current, i_{ss}, and concentration of aqueous transferable ions; the linear fitting and regression equation are given for comparison. Three replicate CVs were collected for each concentration of ions, in which mean and standard deviation (represented as the error bars in each panel) values of i_{ss} were calculated.

Next, we employed the double-potential step chronoamperometry developed in our prior work[3] to further investigate the elusive "nucleation promoter" effect from TEA^+ on Li^+–ionosomes. This method, in essence, is a generation-collection mode for SEE. Firstly, a positive "generation" potential, e.g., 0.9 V at the water/toluene micro-ITIES (refer to Figures 1 and 2), is applied to transfer enough hydrated Li^+ into toluene for a given period of time. Li^+–ionosomes will form at/near the oil side of the ITIES by electrostatic attractions through a unique differential solvation between the hydrated Li^+ and lipophilic bulky TB^-. Afterwards, a reversed constant bias, e.g., 0 V (see Figure 2), is applied immediately to collect the current vs. time (*i*–*t*) curves, which trace numerous stochastic and discrete negative ionic current spikes one after another. The "collection" potential is more negative away from the PZC because Li^+–ionosomes are positively charged water droplets. We believe that the

difference in packing density between small Li^+ and bulky TB^- at the inner and outer sides of the ionic bilayer enclosing the ionosomes causes the breakdown of charge neutrality. We ascribe these discrete current spikes to "kiss and fusion" of the ionosomes on the oil side of the micro-ITIES and the ensuing liberation of their enclosed Li^+ cations from each ionosome. Transfer of clusters of cations from toluene into water generates these downward current spikes, according to the current convention defined in the Experimental Section. Figure 3 shows TEA^+ concentration effect on Li^+–ionosomes. Picoampere (pA) scale short-duration transient current spikes are clearly seen, in which the frequency of collision/fusion events increases as the TEA^+ increases. Specifically, in total 53, 85, and 127 fusions in 150 s were counted for 1 mM, 3 mM, and 5 mM TEA^+, respectively. It corresponds to a fusion frequency of 0.35, 0.57, and 0.85 Hz, respectively. Basically, the fusion frequency is roughly proportional to the square root of TEA^+ concentration. Of course, all these fusion events were recorded in the presence of 10 mM LiCl in aqueous inside the micropipette. In other words, hydrated Li^+ is the essential factor for the nucleation and growth of the ionosomes. However, seen from Figure 3A with only 10 mM LiCl in aqueous, its fusion events is much less (34 events, i.e., 0.23 Hz). So, TEA^+ functions as the "nucleation promoter" for Li^+–ionosomes, as has been discussed above. This observation corroborates our previous findings made at the water/TFT micro-ITIES.[3] The demonstration in Figure 3 signifies another successful application of the micro-ITIES as the sensing platform for SEE. Several groups like Laborda,[23] Samec,[24] Stockmann and Kanoufi,[25] and also ourselves,[3, 26] have participated in the development of SEE that is based on the polarized micro-ITIES.

Then, we performed a statistical analysis of these current spikes. Information on the ionic spike height, diameter, charge, and dwell time of Li^+–ionosomes, in the absence or presence of TEA^+, can be grasped in Figures S5~S8, in the SI. Calculation starts from the charge per spike, i.e., integrating the current as a function of time. Diameter of Li^+–ionosomes is estimated by packing of smaller hydrated Li^+ (radius of 382 pm)[27] spheres in a hexagonal grid on the surface of the water core of the ionosomes. Diameter of TB^- (≈ 1 nm) is included in calculating the size distributions of Li^+–ionosomes.[3] While, spike height and dwell time are read directly from the running software. With only 10 mM LiCl, Gaussian fitting gives modal charge and size values of 126±10 fC and 435±14 nm, respectively. Accordingly, on average Li^+–ionosomes contain 7.86×10^5 Li^+, according to Eq. 3, in which N_{Li^+} is the number of enclosed Li^+ ions per ionosome, Q_{spike} is the charge under an ionic spike, and e is the elementary charge.

$$N_{Li^+} = Q_{spike} / e \qquad (3)$$

The average spike height and dwell time for fusion events of Li^+–ionosomes are 1837±85 fA and 300±8 ms, respectively. Compared to 10 mM LiCl with different concentrations of TEACl (see Figures S6~S8, SI), a notable feature is that the average spike height increases to approximately twice as that without TEA^+ and the dwell time decreases 2-fold instead. With addition of TEA^+, however, the average charge and the corresponding average diameter do not change significantly. Note that a histogram featuring with a more dispersed distribution (i.e., larger standard deviation) fitted with a Gaussian distribution function often leads to a larger error. Besides, since both TEA^+ and Li^+ contribute to the measured ionic current, these estimated values are just rough approximations. Anyway, in the presence of TEA^+, the number of ionosomes with larger size is relatively increased.

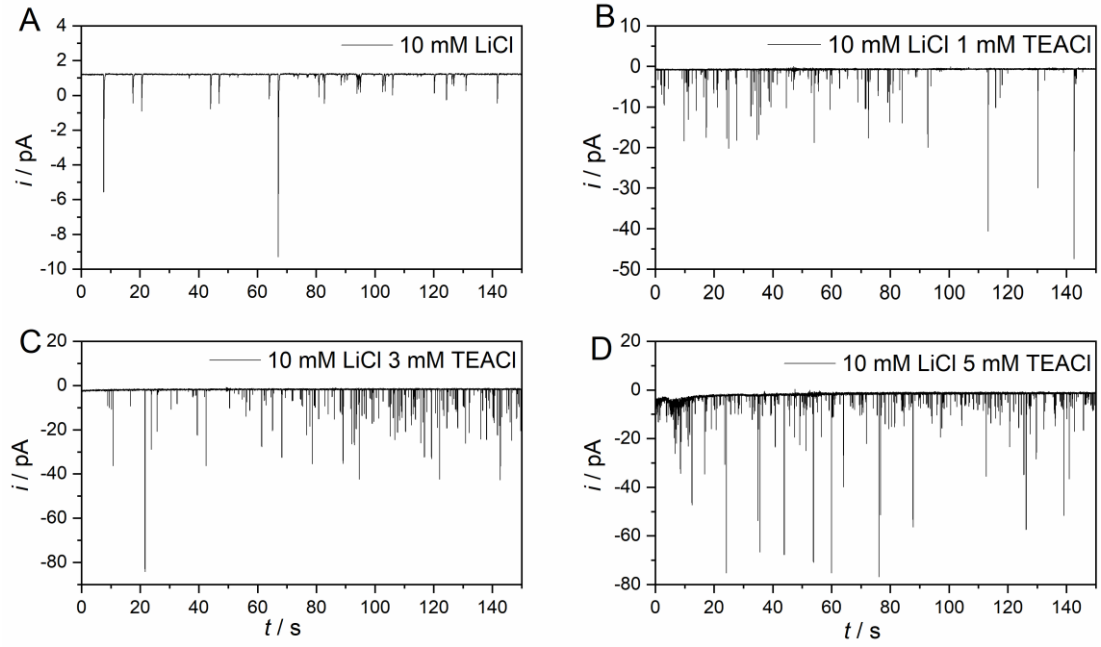

Figure 3. Effect of aqueous TEA^+ concentration. The *i*–*t* curves recorded at 0.006, 0.006, 0.096, and 0.096 V (refer to Figure 2C) for collisions and fusions of Li^+–ionosomes (corresponding to panels A, B, C, and D, respectively), which are formed at 0.996 V (refer to Figure 2C) using the electrochemical cells 1 (for panel A) and 3 (for panels B-D), respectively. Cells 1 and 3 are detailed in Scheme 3.

Figure 4 shows a comparison of size distributions of Li^+–ionosomes formed by electrochemical and chemical polarization. Chemical polarization is the distribution of an antagonistic salt, here LiTB, between water and toluene, under equilibrium. Dynamic light scattering (DLS) gives a distribution interval of 210~520 nm and a modal diameter of ca. 400 nm, which is in fair agreement with the electrochemical results (mainly distributed between 300 and 600 nm). We note that the electrochemical method detects some bigger droplets.

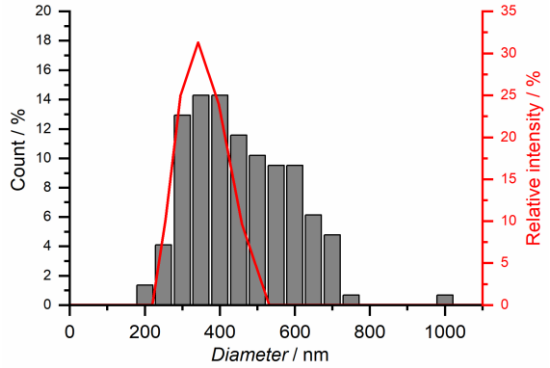

Figure 4. Comparison of the Li^+–ionosomes size distribution obtained via electrochemical polarization (grey bars) and that from DLS measurement via chemical polarization (red line). The histogram is reproduced from Figure S5, panel B, SI.

Next, we employ the bulk electrolysis model to analyze the behavior of an ionic spike per ionosome fusion. Ionic electrolysis commences when a fusion pore forms at the moment of an abrupt kiss between an ionosome and the toluene/water interface. This fires a current spike, followed by an exponential decay with time. Single fusion events of ionosomes with the soft interface mimics the exocytosis of vesicles releasing neurotransmitters in vivo.[28] Figure 5, A to C, gives a quantitative analysis for fusion of an ionosome sized in 393, 365, and 719 nm in

diameter, using Eq. S1, in the SI. Figure 5D displays the blowup of a train of sequential but still disjoining ionic spikes. The experimental data (black squares) aligns perfectly with the theoretical curve (blue line). The fusion pore has a contact radius, r_c, which is assumed to be constant after the kiss of a Li^+–ionosome with the toluene/water micro-ITIES. Note that this simplification helps to gain new physical insights and grasps its nature of the fusion process but might not be the real scenario. Very likely the opening of the fusion pore will expand after its nascent formation due to destructuration of the ionic bilayer, leading to the release of a larger flux of Li^+ into the aqueous phase. The mechanism underpinning this phenomenon is that after kiss with the negatively (water vs. toluene) polarized micro-ITIES, the outer lipophilic counter-ion layer, i.e., the monolayer made of TB^- will be ruptured/collapsed, forming a fusion pore, with the help of electrostatic attraction with the BA^+ monolayer located at the oil side of the micro-ITIES. But, no improvement can be made on this employed model at this stage, as no suitable other in-situ experimental tools can be applicable to elucidate more details. Besides, we found that a 10-fold smaller diffusion coefficient of Li^+ in water employed in the fitting could result in an acceptable and reasonable contact radius. If the pristine diffusion coefficient of Li^+ in water, 1.03×10^{-9} m^2 s^{-1},[29] was used instead, an unrealistic contact radius that is smaller than that of a bare Li^+ (59 pm in radius)[29] could be obtained from the best fit for a Li^+–ionosome of ≤ 250 nm in diameter, for example. We decided to use smaller diffusion coefficient of Li^+ for modelling, also because the rate-determining step for a Li^+–ionosome fusion might be identified as the dissociation of LiTB and the accompanying diffusion away of very bulky TB^- in toluene (see Scheme 2). The perfect agreement between theory and experiment reconciles the hypotheses which seem unreasonable and stated above. In general, the contact radius increases as the size of a Li^+–ionosome increases (Figure 5, A to C), in good line with our prior findings.[11a, 11b] The best-fit parameters of two other modellings, along with the aforementioned three cases (Figure 5, A to C), are listed in Table 1.

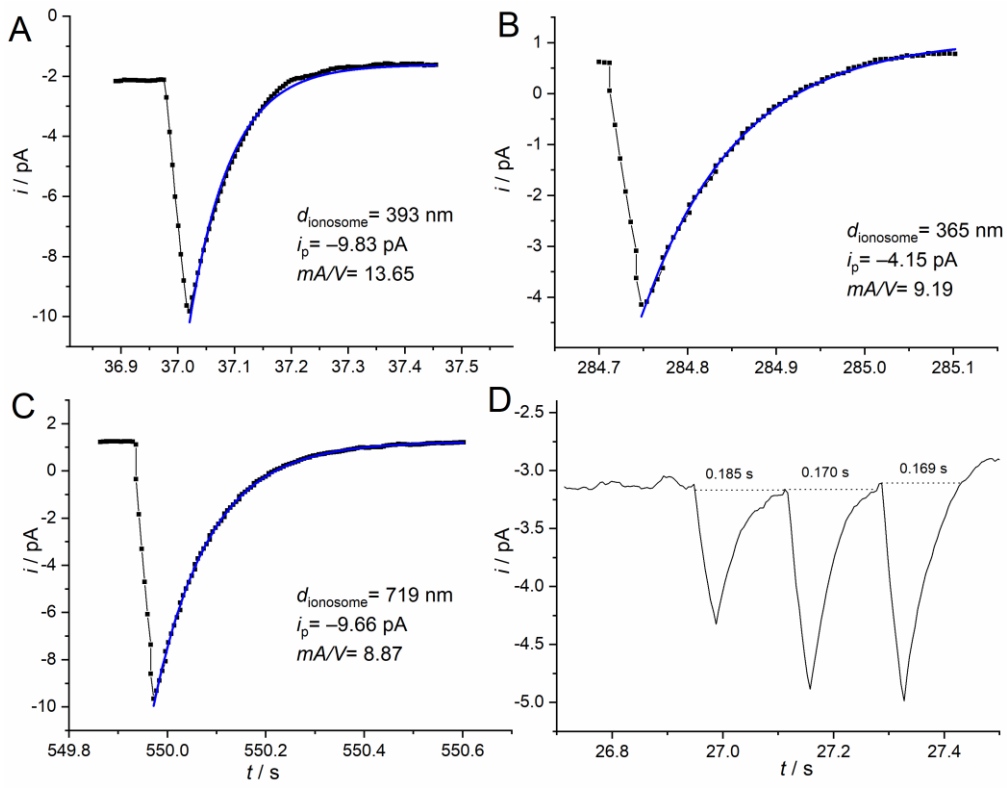

Figure 5. Zoom-in *i*–*t* ranges of (A) 36.9~37.45 s, (B) 284.7~285.1 s, (C) 549.85~550.6 s, and (D) 26.7~27.5 s of Figure S9 in the SI. The experimental data were sampled every 5 ms (black squares). The fitted *i*–*t* curve (blue line, in panels A-C) was obtained using the bulk electrolysis model (Eq. S1, SI).

Table 1. Summary of the *i*–*t* best-fit parameters of Li^+–ionosomes with varying sizes.

Diameter (nm)	V (m^3)	mA/V (s^{-1})	r_c (nm)
365	2.55E–20	9.19	0.568
393	3.18E–20	13.65	1.05
719	1.95E–19	8.87	4.19
783	2.51E–19	8.85	5.40
842	3.12E–19	8.98	6.81

Conclusion

In summary, the in-situ generation and detection of single Li^+–ionosomes that bear a net charge is demonstrated at the micro-ITIES between water and toluene, a truly apolar medium with low dielectric constant. The ionosome is another new category of nano-/microemulsion, the nanoscopic ionic-bilayer encapsulated water droplets. Besides the canonical organic solvents including DCE, nitrobenzene, and 2-nitrophenyl octyl ether (NPOE) that are used widely in the ITIES electrochemistry, well-defined ion-transfer voltammograms at a water/toluene interface have been observed in the present work. This achievement is enabled with the help of the miniaturization of the interface and the high solubility of TDDATB in toluene. The relevant PPW spans ca. 0.9 V at the water (10 mM LiCl)/toluene (20 mM TDDATB) interface. The available organic media for dispersing spontaneously generated ionosomes via either electrochemical or chemical polarization have extended from TFT and DCB to toluene. “Nucleation promoter” effect of quaternary ammonium cations with different alkyl chain length and with different concentration and our attempted fitting of ionic spikes with the bulk electrolysis model shed new light on the mechanism of ionosomes. Some other work, like the promoting effect from other more hydrophilic cations (e.g., ammonium and cesium cations) on Li^+–ionosomes are required to further elucidate the underlying physical principles. This work spurs the advancement of colloidal science, ITIES electrochemistry, and SEE.

Experimental Section

Chemicals. All the chemicals were used as received without further purification unless otherwise stated. Toluene (≥99.5%), lithium chloride (LiCl, ≥99%), lithium perchlorate ($LiClO_4$, 99.99%), Lithium tetrafluoroborate ($LiBF_4$, 99.99%), sodium chloride (NaCl, 99.5%), and potassium chloride (KCl, ≥99%) were purchased from Aladdin. Potassium tetrakis(pentafluorophenyl)borate (KTB, 97%), ammonium chloride (NH_4Cl, 99.99%), tetrapropylammonium chloride (TPrACl, 97%), lithium bis(trifluoromethanesulfonyl)imide (LiTFSI, 99.9%), 300-400 mesh silica gel, and anhydrous magnesium chloride ($MgCl_2$, 99%) were obtained from Macklin. Lithium tetrakis(pentafluorophenyl)borate diethyl etherate (LiTB) was provided from Boulder Scientific, US. Hydrochloric acid (HCl, 36−38%) and sulfuric acid (H_2SO_4, 98%) were bought from Xilong Scientific (Shantou, China). Tetramethylammonium chloride (TMACl, ≥98%), tetraethylammonium chloride (TEACl, 98%), hydrogen

peroxide solution (H_2O_2, 3% w/w), and tetradodecylammonium bromide (TDDABr, ≥99.0%) were sourced from Sigma-Aldrich. The lipophilic salt of tetradodecylammonium tetrakis(pentafluorophenyl)borate (TDDATB) used as the supporting electrolyte in toluene was prepared by metathesis between TDDABr and KTB, followed by a purification (silica gel chromatography followed by rotary evaporation) process.[30] Silver (Ag, 99.9985%, temper: annealed, 250 µm in diameter) wire was bought from Alfa Aesar. All aqueous solutions were prepared with a Millipore-Q ultrapure water (≥ 18.2 MΩ cm). A PHS-3C pH meter (Lei-Ci Co., Shanghai, China) was used to measure pH in aqueous solutions.

Micropipette Fabrication and Characterization. The micropipettes were pulled with a PC-100 puller (Narishige Instrument, Japan) using borosilicate glass capillaries (1 mm outer diameter, 0.58 mm inner diameter, 10 cm length, with filament; Sutter Instrument, US). Throughout the work presented herein, the ITIES was supported at the orifice of a micropipette with a typical inner diameter (i.d.) of ~2 µm. Preparing such a micropipette applies the one-stage pulling parameters: No. 1 Heater Level: 59-69, number of load-bearing weights: 2-4. Prior to pulling, inside of the capillaries was cleaned with a fresh piranha solution (Note that use of the piranha solution requires extreme care) followed by a thorough rinse with a copious amount of water and dehydration in the oven. The micropipette tip morphology, taper angle, and size were inspected by either a metallographic optical microscope (model: IE31, Mshot Co., Guangzhou, China) or a field-emission high-resolution scanning electron microscope (SEM, Hitachi SU 8100, Japan, 10.0 kV accelerating voltage). A gold nanofilm was sputtered on the shank part of a micropipette for SEM imaging, minimizing the charging effect.

Electrochemical Measurements. All of electrochemical measurements were conducted using a CHI model 760E potentiostat (CH Instruments, Shanghai, China) in a two-electrode one-compartment electrolytic cell housed in a Picoamp Booster embedded Faraday cage (CHI200B, CH Instruments, Shanghai, China). The working electrode is an aqueous electrolyte-filled micropipette, in which a 250 µm-diameter Ag/AgCl or Ag/Ag_2SO_4 wire was inserted and used for electrical connection with the potentiostat. We filled the micropipettes with aqueous electrolyte solutions by a small syringe (10 µL, World Precision Instruments). Another Ag/AgCl wire but with a diameter of 600 µm was positioned within the outer toluene solution, functioning as the counter/pseudo-reference electrode (CE/PRE). Ag/AgCl wire was prepared by electrolysis of an Ag wire in 1 M HCl solution under +1.5 V potentiostatic conditions for 10 min, with a Pt wire as the CE/RE. Ag/Ag_2SO_4 wire was made in the same way but in 50 mM H_2SO_4 aqueous solution. Note that the current was recorded as positive when cations transferred from aqueous into the organic solution or anions transferred from organic into the aqueous solution, obeying the IUPAC convention. The biased potential was corrected to the Galvani potential scale, according to the formal transfer potential of either TMA^+ or TEA^+ at water/toluene interface.[11c]

Ionosomes Formed by Chemical Polarization. The spontaneously formed ionosomes via chemical polarization (i.e., biphasic distribution of an antagonistic salt) were sized by dynamic light scattering (DLS) with a Mastersizer 2000 instrument (Malvern, UK). Chemical polarization was carried out after 24 h from the initial contact between 10 mL of 5 mM LiTB in water (lower phase) and 2 mL of toluene (upper phase) in a glass vial.

Acknowledgements

This work was supported by the National Natural Science Foundation of China (Nos. 21904143, 22108085, 22102025) and the Fundamental Research Funds for the Central Universities, Sun Yat-sen University, 2021qntd13. This work has also partially emanated from the research of P.P. supported by the European Research Council through a Starting Grant (agreement no. 950038). P.P. also gratefully acknowledges the Academy Research Fellow funding (Grant No. 315739) by the Academy of Finland and the Academy of Finland project funding for PHOTOH2 (Grant No. 334828).

Keywords: single-entity electrochemistry • ionosomes • toluene • ITIES • bulk electrolysis

References

[1] D. J. Shaw, in *Introduction to Colloid and Surface Chemistry (Fourth Edition)* (Ed.: D. J. Shaw), Butterworth-Heinemann, Oxford, **1992**, pp. 262-276.

[2] D. Michler, N. Shahidzadeh, M. Westbroek, R. van Roij, D. Bonn, *Langmuir* **2015**, *31*, 906-911.

[3] H. Deng, P. Peljo, X. Huang, E. Smirnov, S. Sarkar, S. Maye, H. H. Girault, D. Mandler, *J. Am. Chem. Soc.* **2021**, *143*, 7671-7680.

[4] G. C. Gschwend, A. Olaya, H. H. Girault, *Chem. Sci.* **2020**, *11*, 10807-10813.

[5] aH. Deng, P. Peljo, T. J. Stockmann, L. Qiao, T. Vainikka, K. Kontturi, M. Opallo, H. H. Girault, *Chem. Commun.* **2014**, *50*, 5554-5557; bA. Trojánek, J. Langmaier, H. Kvapilová, S. Záliš, Z. Samec, *J. Phys. Chem. A* **2014**, *118*, 2018-2028.

[6] aI. Benjamin, *Science* **1993**, *261*, 1558-1560; bN. Kikkawa, L. Wang, A. Morita, *J. Am. Chem. Soc.* **2015**, *137*, 8022-8025.

[7] P. Sun, F. O. Laforge, M. V. Mirkin, *J. Am. Chem. Soc.* **2007**, *129*, 12410-12411.

[8] A. J. Gotch, G. W. Loar, A. J. Reeder, E. E. Glista, *Langmuir* **2008**, *24*, 4485-4493.

[9] P. N. Sturzenegger, U. T. Gonzenbach, S. Koltzenburg, L. J. Gauckler, *Soft Matter* **2012**, *8*, 7471-7479.

[10] aM. Brust, M. Walker, D. Bethell, D. J. Schiffrin, R. Whyman, *J. Chem. Soc., Chem. Commun.* **1994**, 801-802; bA. Uehara, S. G. Booth, S. Y. Chang, S. L. M. Schroeder, T. Imai, T. Hashimoto, J. F. W. Mosselmans, R. A. W. Dryfe, *J. Am. Chem. Soc.* **2015**, *137*, 15135-15144.

[11] aH. Deng, J. E. Dick, S. Kummer, U. Kragl, S. H. Strauss, A. J. Bard, *Anal. Chem.* **2016**, *88*, 7754-7761; bC. Liu, P. Peljo, X. Huang, W. Cheng, L. Wang, H. Deng, *Anal. Chem.* **2017**, *89*, 9284-9291; cM. Kasuno, Y. Matsuyama, M. Iijima, *ChemElectroChem* **2016**, *3*, 694-697; dM. Kasuno, K. Wakabayashi, Y. Matsuyama, R. Yamamura, *Electrochim. Acta* **2020**, *343*, 136069.

[12] F. O. Laforge, P. Sun, M. V. Mirkin, *J. Am. Chem. Soc.* **2006**, *128*, 15019-15025.

[13] H. D. Jetmore, C. B. Milton, E. S. Anupriya, R. Chen, K. Xu, M. Shen, *Anal. Chem.* **2021**, *93*, 16535-16542.

[14] P. J. Rodgers, S. Amemiya, *Anal. Chem.* **2007**, *79*, 9276-9285.

[15] Q. Li, S. Xie, Z. Liang, X. Meng, S. Liu, H. H. Girault, Y. Shao, *Angew. Chem., Int. Ed.* **2009**, *48*, 8010-8013.

[16] F. Li, Y. Chen, M. Zhang, P. Jing, Z. Gao, Y. Shao, *J. Electroanal. Chem.* **2005**, *579*, 89-102.

[17] T. Wandlowski, V. Mareček, Z. Samec, *Electrochim. Acta* **1990**, *35*, 1173-1175.

[18] M. Ue, *J. Electrochem. Soc.* **1994**, *141*, 3336-3342.

[19] T. Osakai, K. Ebina, *J. Phys. Chem. B* **1998**, *102*, 5691-5698.

[20] aN. Dubouis, C. Park, M. Deschamps, S. Abdelghani-Idrissi, M. Kanduč, A. Colin, M. Salanne, J. Dzubiella, A. Grimaud, B. Rotenberg, *ACS Central Science* **2019**, *5*, 640-643; bX. Wang, T. S. Mathis, Y. Sun, W.-Y. Tsai, N. Shpigel, H. Shao, D. Zhang, K. Hantanasirisakul, F. Malchik, N. Balke, D.-e. Jiang, P. Simon, Y. Gogotsi, *ACS Nano* **2021**, *15*, 15274-15284.

[21] Y. Marcus, *J. Chem. Soc., Faraday Trans.* **1991**, *87*, 2995-2999.

[22] Y. Naito, W. Murakami, K. Eda, M. Yamamoto, T. Osakai, *J. Phys. Chem. B* **2015**, *119*, 6010-6017.

[23] E. Laborda, A. Molina, V. F. Espín, F. Martínez‐Ortiz, J. G. d. l. Torre, R. G. Compton, *Angew. Chem., Int. Ed.* **2017**, *56*, 782-785.

[24] aA. Trojánek, V. Mareček, Z. Samec, *Electrochem. Commun.* **2018**, *86*, 113-116; bA. Trojánek, Z. Samec, *Electrochim. Acta* **2019**, *299*, 875-885.

[25] aT. J. Stockmann, L. Angelé, V. Brasiliense, C. Combellas, F. Kanoufi, *Angew. Chem., Int. Ed.* **2017**, *56*, 13493-13497; bT. J. Stockmann, J.-F. Lemineur, H. Liu, C. Cometto, M. Robert, C. Combellas, F. Kanoufi, *Electrochim. Acta* **2019**, *299*, 222-230.

[26] L. Huang, J. Zhang, Z. Xiang, D. Wu, X. Huang, X. Huang, Z. Liang, Z.-Y. Tang, H. Deng, *Anal. Chem.* **2021**, *93*, 9495-9504.

[27] E. R. Nightingale, *J. Phys. Chem.* **1959**, *63*, 1381-1387.

[28] C. Amatore, S. Arbault, M. Guille, F. Lemaître, *Chem. Rev.* **2008**, *108*, 2585-2621.

[29] P. W. Atkins, *Physical Chemistry, 4th ed.*, Oxford University Press, Oxford, **1990**.

[30] M. L. Colombo, J. V. Sweedler, M. Shen, *Anal. Chem.* **2015**, *87*, 5095-5100.

Entry for the Table of Contents

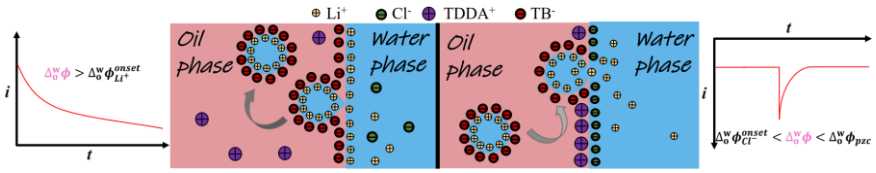

A hydrophobic ionic liquid, $TDDA^{+}TB^{-}$, highly soluble in toluene, enables a polarizable interface with an aqueous solution with $Li^{+}Cl^{-}$ dissolved. The water/toluene micro-interface is polarized at potentials more positive than the onset potential for Li^{+} transfer to drag hydrated Li^{+} into toluene, waiting for Li^{+}–ionosomes assembly. Reversing the electric field unveils a train of quantized ionic current spikes that are relevant to the single fusion events of Li^{+}–ionosomes with the interface.